Article:

Aminu, I, Nahil, MA and Williams, PT orcid.org/0000-0003-0401-9326 (2020) Hydrogen from Waste Plastics by Two-Stage Pyrolysis/Low-Temperature Plasma Catalytic Processing. Energy & Fuels, 34 (9). pp. 11679-11689. ISSN 0887-0624

https://doi.org/10.1021/acs.energyfuels.0c02043

Hydrogen from waste plastics by two-stage pyrolysis/low temperature plasma-catalytic processing

Idris Aminu, Mohamad A. Nahil, Paul T. Williams*

School of Chemical & Process Engineering, University of Leeds, Leeds, LS2 9JT, UK

*Corresponding author(Email; p.t.williams@leeds.ac.uk; Tel; #44 1133432504)

ABSTRACT

Hydrogen was produced from waste plastic (polyethylene) using a novel two-stage pyrolysis-low temperature (250 °C) plasma catalytic steam reforming process. Pyrolysis of the polyethylene generated pyrolysis gases which were catalytically steam reformed in the presence of low temperature non-thermal plasma (dielectric barrier discharge) to produce hydrogen gas. In the absence of catalyst, increasing the plasma power resulted in a significant increase in hydrogen yield. Different catalysts (Ni/Al_2O_3, Fe/Al_2O_3, Co/Al_2O_3 and Cu/Al_2O_3) were incorporated in the discharge region of the plasma reactor and the Ni/Al_2O_3 produced the highest yield of hydrogen at 1.5 mmol $g^{-1}_{plastic}$. Addition of steam to the plasma catalytic process was investigated at different steam weight hourly space velocities (WHSV) using the Ni/Al_2O_3 catalyst. The addition of steam to promote catalytic steam reforming reactions resulted in a marked increase in hydrogen yield, producing the highest hydrogen yield of 4.56 mmol $g^{-1}_{plastic}$ at a WHSV of 4 g h^{-1} $g^{-1}_{catalyst}$.

Key words: Pyrolysis; Steam reforming; Plasma; Hydrogen; Plastic

INTRODUCTION

Increasing demand for plastic products, due to their suitability for a wide range of applications, has resulted in an increasing amount of waste plastics generated each year [1]. The majority of the plastics produced are designed for single use and become waste almost immediately after use, resulting in environmental and waste management issues [2]. Geyer et al. [3] studied the production, use and fate of all plastics ever made from 1950-2015. They estimated that by 2015, a total of about 8.3 billion tonnes of plastic (resins, fibres and additives) was produced out of which 2.5 billion tonnes is still in use while 5.8 billion tonnes have become accumulated waste. Environmental issues arise due to the accumulation of waste plastic in the environment, for example, toxic additives contained within historical plastics, marine micro-plastics and illegal and unsightly dumping of waste plastics [4-6].

Waste plastics have received increasing interest by researchers as alternative sources of high value products through thermal processing methods such as pyrolysis and gasification [7-10]. Among these high value products, hydrogen is of current interest because it is a carbon-free clean fuel that produces only water as the by-product of its combustion. Hydrogen is also used in several industrial applications such as ammonia production, methanol production, electricity generation and fuel production. Currently, hydrogen is mainly produced from fossil fuels via natural gas (methane) steam reforming typically using nickel-based catalysts at high temperature (700 - 1000 °C) and pressure (0.3 – 2.5 MPa). Producing hydrogen from waste plastics would provide an alternative feedstock in addition to solving an environmental waste plastics management issue. Building on the commercial methane steam reforming process, several research groups have developed a two-stage process where the plastics are pyrolysed to produce a range of hydrocarbon gases, which then pass to a second stage where catalytic steam reforming of the hydrocarbons takes place to produce a hydrogen-rich gas [11-18]. Such studies have been carried out to maximize the hydrogen production by investigating the effects of the operating parameters such as temperature, steam input, pressure, residence time, etc. [11-14]. In addition, different types of catalysts have been developed for the pyrolysis gas steam reforming process aimed at enhanced catalytic activity towards hydrogen production and to minimise catalyst coke formation [15-18]. However, the challenges to these plastics pyrolysis-catalytic reforming processes include the high catalyst temperatures involved (typically ~800 °C) and consequent energy requirement and catalyst deactivation due to carbonaceous coke deposition on the catalyst.

These challenges can be overcome by the development of a new process which uses low temperature non-thermal plasma technology. This technology may provide a promising alternative to the thermal catalytic process for the conversion of wastes into value added chemicals and fuels at low temperatures. Thermal plasma operates at high temperature (10,000-100,000 K) [19-22], but non-thermal plasma operate at much lower temperature (e.g.~250 °C). Non-thermal plasmas consist of particles at different temperatures and degrees of freedom. Electron temperature determines the ionization and the chemical processes in this type of plasma [21]. Most of the plasma chemical reactions occur through electron impact reactions such as electron impact excitation, dissociation and ionization. The collisions between the high temperature electrons and the relatively cold gas molecules in non-thermal plasmas result in generation of radicals such as atomic oxygen, hydroxyl and excited oxygen, that can influence the kinetics of chemical conversion reactions [20]. These radicals are able to break most chemical bonds and allow reactions that are thermodynamically unfavourable to occur at low temperatures. This has enabled non-thermal plasmas to be used for the synthesis of fuels and chemicals [23]. In non-thermal plasmas, the ionization processes induced by an electric field dominate the thermal processes and produce relatively high-energy electrons as well as excited ions, atoms and molecules. The average electron density in a non-thermal plasma is very high, typically 1 – 10 eV, while the bulk temperature remains as low as room temperature [21]. This non-equilibrium property of the non-thermal plasma makes it chemically selective and can be used for catalytic processes [24]. The non-thermal plasma process has been used by researchers for gas conversions, and different experimental parameters have been studied [25-27].

The addition of a catalyst to the plasma can have a synergistic effect resulting from the interactions between the plasma and the catalyst to enhance the conversion of the feedstock, improve selectivity of the desired product, increase energy efficiency of the process and prevent catalyst deactivation by reducing catalyst coking [28,29]. The interaction is interdependent with the plasma, modifying the properties of the catalyst such as its dielectric constant, surface faceting and morphology, while the catalyst modifies the electric field generation and distribution and the electron energy distribution which affect the generation of reactive species [30]. Studies have been carried out using plasma-catalysis which have shown that the synergistic reactivity is improved over the performance of either plasma alone or the conventional catalytic process alone [31-34]. Others have shown that the packing mode of the catalyst material and the position of the catalyst can influence the conversion process [35,36]. This suggests that synergy is not always achieved and depends on experimental conditions, catalyst selection and packing mode which should be investigated to get a better understanding of the synergistic effects of the plasma-catalysis process.

Different types of non-thermal plasmas have been studied for gas conversion processes including dielectric barrier discharge (DBD) [37,38], corona discharges [39,40], gliding arc discharge [41,42] and glow discharges [43,44]. Among them, the dielectric barrier discharge (DBD) plasma is attracting interest because it simple design, easy scale up and low installation cost [45]. The discharge in a DBD plasma can be generated in the annular gap between two co-axial electrodes one of which is shielded from the gas by dielectric materials.

Non-thermal plasma-catalysis has been used in several applications to produce syngas from a simulated biogas [46], for reforming of toluene as a model for biomass tar [47,48] and for the production of hydrogen from biomass pyrolysis gases [49]. However, to the best of the authors knowledge, no previous work has been reported on the use of non-thermal plasma-catalysis for reforming of pyrolysis products from plastic waste. In this paper, the production of hydrogen-rich syngas from waste high density polyethylene (HDPE) was studied using a novel two-stage pyrolysis-non-thermal plasma reactor. Pyrolysis of the waste plastic takes place in the first stage reactor and the pyrolysis gases are passed to the second stage, low temperature, non-thermal DBD plasma reactor. The influence of different plasma-catalysis process conditions and the influence of different catalysts were investigated with the aim of producing a hydrogen-rich gas.

MATERIALS AND METHODS

Materials: The waste plastic used in this study was high density polyethylene (HDPE), one of the major plastics found in municipal solid waste. It was obtained as a post-consumer recycled waste plastic of 2 mm sized pellets from Regain Polymers Ltd., UK. Ultimate analysis of the HDPE revealed that it had an elemental content of 81.78% carbon, 10.59% hydrogen and 0.54% nitrogen and a calorific value of 28.06 $MJkg^{-1}$. Proximate analysis showed a moisture content of 0.14%, volatile matter of 97.84%, fixed carbon 0.16% and ash 3.63%.

For the plasma catalysis, 10% nickel alumina catalyst (10 wt.% Ni/Al_2O_3) was the main catalyst used for the investigation of the influence of process parameters on hydrogen yield. In addition, and for comparison, three other transition metal catalysts (Fe/Al_2O_3, Co/Al_2O_3 and Cu/Al_2O_3) were also used. All the catalysts were prepared by the wet impregnation method to give a 10 wt.% metal loading followed by calcination and reduction. In each case, a measured amount of the metal nitrate hexahydrate was dissolved in deionised water and stirred with a magnetic stirrer for 30 minutes. A measured quantity of alumina pellets (1mm diameter) was then added and the mixture heated to 60 °C with continuous stirring. The catalyst precursor was then dried overnight in an oven at 105 °C and then calcined at 750 °C by heating in air from ambient to 750 °C with 20 °C min^{-1} heating rate and held for 3 h at 750 °C. This was then followed by reduction of the catalyst under a reducing environment of hydrogen in nitrogen (5% H_2 in 95% N_2) at 800 °C with a heating rate of 20 °C min^{-1} for two hours.

Experimental system: A schematic diagram of the two-stage pyrolysis-plasma reactor used in this study for hydrogen production is shown in Figure 1. Figure 2 shows a detailed schematic diagram of the pyrolysis reactor coupled with the plasma reactor showing the insulation and electrode system. This two-stage system has the advantage of independently monitoring and controlling the conditions in each reactor and also improves the contact between pyrolysis gases and the catalyst. The first stage pyrolysis reactor holds the waste plastic sample and the second stage holds the catalyst within a dielectric barrier discharge (DBD) reactor. The first stage pyrolysis reactor was constructed of stainless steel which was a fixed bed reactor, 250 mm in length by 20 mm internal diameter, heated using a controlled electrical furnace with programmable temperature control. A stainless steel crucible holds the HDPE sample, suspended in the middle of the reactor. The pyrolysis reactor was heated to a final temperature of 500 °C at a heating rate of 20 °C min^{-1} to generate pyrolysis gases from the thermal degradation of the waste plastic. The pyrolysis reactor was held at 500 °C for a further 15 minutes. The pyrolysis and plasma reactors are connected using a electrically insulating ceramic transfer tube. The second stage DBD plasma reactor consisted of an outer electrode made of an 80 mm long copper mesh wrapped around a quartz tube of 25 mm o.d. and 22 mm i.d. The inner electrode was an 18mm stainless steel rod centrally placed in the quartz tube thus making a discharge length of ~80 mm and discharge gap of 2 mm. The inner electrode was connected to an AC high-voltage power supply (0 – 240V) with a frequency of 1500 Hz and a maximum peak to peak voltage of 20 kV while the outer electrode was connected to earth. The catalyst was held by quartz wool in the space between the inner electrode and the inner wall of the quartz tube at the centre of the discharge zone in the second stage reactor. High voltage was applied to the packed bed where a non-equilibrium plasma will be created in the void space between the dielectric pellets of the catalyst bed. By refraction of the electric field on the pellets, the electric field becomes non-uniform and stronger with an intensity dependent on the porosity, shape and dielectric constant of the pellets. The discharge power supplied to the plasma was kept constant throughout the experiment by adjusting the input voltage. All electrical signals were monitored using a mixed domain digital oscilloscope (Tektronix MDO3024). Distilled water was injected into the second stage plasma-catalysis reactor using a glass syringe controlled by a metered pump to generate steam for the catalytic reforming of the pyrolysis gases. The quartz reactor was held in an electrical furnace maintained at 250 °C. This temperature was chosen to minimise condensation of product pyrolysis gases and input steam. Nitrogen gas continuously purged the reactor system and the product gases from the second reactor which passed to a series of glass condensers cooled by dry ice where the condensable products are collected. The non-condensable gases were passed to a 25 L Tedlar^{TM} gas sample bag for later analysis in a suite of packed column gas chromatographs.

The experimental procedure involved pre-heating and maintaining the second stage plasma reactor at 250 °C. Once the second stage reactor temperature was stabilised, the pyrolysis heating was commenced. When the pyrolysis process reached a temperature of 200 °C, the plasma system was then powered up to generate the plasma. Steam injection commenced when the pyrolysis temperature reached 120 °C.After completion of pyrolysis, the liquid and gas products were collected for a further 20 minutes to ensure all the pyrolysis products from the first stage have reacted in the plasma reactor. At the end of the experiment, the solid residue retained in the sample crucible and the condensed liquids collected in the condenser system were weighed for determination of the mass balance. The gas in the gas sample bag was analysed for the identification and quantification of the product gas composition and converted to mass to obtain the total gas yield. All experiments were repeated at least twice for accuracy with negligible differences between the repeated experiments. Results were the average of the repeated experiments.

Gas analysis: The gases collected in the gas sample bag were immediately analysed off-line in three separate packed-column gas chromatographs. Hydrocarbons (C_1 – C_4) were analysed using a Varian CP-3380 gas chromatograph equipped with a flame ionisation detector (GC/FID) and a 2m x 2mm column packed with 80 – 100 mesh Hayesep packing material and nitrogen was the carrier gas. The temperature programme started at 60 ºC for 3 min and increased at 20 ºC min^{-1} up to 120 ºC and held for 10 minutes. Permanent gases (H_2, O_2, N_2 and CO) were analysed using another Varian 3380 gas chromatograph with thermal conductivity detector (GC/TCD), 60 – 80 molecular sieve column held at 30 °C and argon carrier gas. CO_2 was analysed using a third Varian 3800 gas chromatograph with a 2m x 2 mm column, but with a different packing material, 80 – 100 mesh Hayesep, and argon carrier gas. The different packing material enabled separation of CO and CO_2 which tend to elute from the column closely together. The gas yield was determined accurately by analysis and calculation, rather than by difference; knowing the nitrogen purge gas flow rate, the volumetric composition and concentration of each of the gases in the gas sample bag coupled with the Ideal Gas Law and known density of each gas, the determination of the mass of each gas and thereby the total mass of gas could be calculated. The product gases were analysed for N_2, O_2, H_2, CO, CO_2, CH_4, C_2H_6, C_2H_4, C_3H_8, C_3H_6, C_4H_{10}, C_4H_8 ,C_4H_6. Extended repeatability experiments were carried out under the same conditions and produced repeatable gas analysis results which gave a standard deviation between 0% and 5% depending on the particular gas.

RESULTS AND DISCUSSION

Influence of plasma on the process: The effect of the non-thermal plasma on the waste plastic pyrolysis gases in relation to hydrogen yield was investigated with the use of plasma alone (no catalyst), plasma-catalysis, plasma-steam reforming and plasma catalytic steam reforming. The experiments were carried out at a pyrolysis temperature of 500 °C in the first stage and using a power input of 60 W to sustain the discharge in the second stage reactor which was maintained at 250 °C. A steam flow rate of 4 $g\ h^{-1}\ g^{-1}_{catalyst}$ was used in the steam reforming experiments and 1g of 10 wt.% Ni/Al_2O_3 catalyst calcined at 750 °C was used in the catalytic processes. The results were compared with that of pyrolysis-catalysis (no plasma). The yield and composition of the gases is based on an input of plastic and water (in the case of steam reforming) and output of product gas, liquid (pyrolysis oil and water) and solid residue. In this work the interest was in the gas only which was determined accurately by mass. The liquid, which is a mixture of oil and water, was not analysed but merely weighed for material balance. The solid char residue was the same for every experiment at 4.0 wt.%, since the same mass of high density polyethylene was used each time and was unaffected by any variables in the second stage plasma-catalytic reactor.

The results in Table 1 show that compared to catalysis alone (10 wt. % Ni/Al_2O_3, no plasma), using plasma in the second stage increased the gas yield from 8.0 wt.% to 10.9 wt.%. This indicates that reactive species have been generated in the plasma which cracked more of the high molecular weight pyrolysis gases into lower molecular weight gas. The non-thermal plasma has been reported to generate electrons with higher energy than the dissociation energies of the C-H and the C-C bonds [21]. It may be suggested that these energetic electrons together with other active species generated in the plasma enhanced the cracking of the HDPE pyrolysis volatiles resulting in increased gas yield. Diaz [24] suggested that the collision between the reactive species and the pyrolysis volatiles lead to the formation of carbenium-like ions and radicals along the hydrocarbon chains which promotes reaction pathways similar to secondary β-scission reactions. In their review on plasma performance of dry reforming of methane (DRM), Chung and Chan [50] noted that electron impact excitation and dissociation (Eqs 1-3) play an important role in the DRM since the direct dissociation of CH_4 in an atmospheric pressure plasma is limited due to high energy requirement. However, Neyts et. al. [51], noted that vibrational energy has an important role in the CH_4 dissociation in a plasma environment. Some of the vibrational energy can be used to reduce the energy barrier of the reaction and on the other hand the vibrationally excited species can have a lower activation barrier than the ground state species. In addition, the plasma species create alternative reaction pathways towards product formation [52].

$$e + CH_4 \rightarrow e + CH_3 + H \qquad (1)$$

$$e + CH_4 \rightarrow e + CH_2 + H_2 \qquad (2)$$

$$e + CH_4 \rightarrow e + CH + H_2 + H \qquad (3)$$

It is suggested that the reactions in this work also followed a similar route where cracking of the hydrocarbons was mainly through dissociation of excited species. In addition to the electron induced chemical reactions, thermochemistry may also exist in the plasma-assisted processes since the collision between the electrons is non-reacting which inevitably transfers energy to the surrounding gas molecules resulting in increased gas temperature [53]. Therefore, even though the furnace temperature of the plasma reactor in this work was ~250 ^{o}C, the temperature inside the plasma-catalyst reaction zone could be much higher [52].

Compared to plasma alone and catalysis alone, plasma-catalysis showed a better performance in terms of total gas yield of 12.0 wt.%. Introducing catalyst in the discharge zone enhanced the average electron energy and electron temperature, resulting in an improved reaction performance [30]. The catalyst also provides a surface for the plasma species to react with the pyrolysis volatiles thereby enhancing the gas yield. It has been reported that adsorption of the species onto the catalyst surface is enhanced by the non-equilibrium nature of the discharge due to vibration excitation, thus increasing the reactivity for the process [29]. When steam was injected for plasma reforming without catalyst, a further increase in the gas yield to 17.0 wt.% was observed possibly because the plasma cracks both the hydrocarbons and the injected steam. It has been reported that addition of steam into the DBD plasma generates H and OH radicals leading to the formation of more hydrogen gas [48].

Using a 10 wt. % Ni/Al_2O_3 catalyst and steam at 4 g h^{-1} $g^{-1}_{catalyst}$ for plasma catalytic steam reforming produced the highest gas yield of 19.8 wt.%. The increased performance when catalyst was used for plasma-catalysis and plasma catalytic steam reforming are suggested to be due to synergistic effects between plasma and the catalyst. It is noteworthy that Ni/Al_2O_3catalyst is active at high temperatures around 800 °C and when used in low temperature reactions, its activity is low [54]. However, the results of the plasma catalysis shown in Table 1 suggests that the catalyst has been activated to some extent by the plasma at the low experimental temperature. When the plasma is in contact with the catalyst surface, it can heat the catalyst surface through the impact of plasma species (charge carries, metastable, photons and excited neutrals), and fast ground state neutral species, and through exothermic reactions [51]. Nozaki et al. [55], studied the steam reforming of methane using a barrier discharge with Ni/SiO_2 catalyst and observed that the vibrational temperature was significantly increased in the presence of the nickel catalyst which resulted in an increased reactivity of the vibrationally excited species. Fridman and Kennedy [56] noted that in a plasma characterised by vibrational-translational equilibrium, the surface temperature can be much greater than the translational gas temperature. When the surface area of the catalyst is so high, this can make the catalyst surface to be preferentially heated without heating the bulk gas. Other studies comparing plasma-alone, catalysis-alone, and plasma-catalysis also reported plasma-catalysis having better performance than plasma alone or catalysis alone [57]. Wang et al. [30], suggested that the interaction between the plasma and the catalyst is interdependent in that the plasma modifies the properties of the catalyst such as dielectric constant, surface faceting and morphology, while the catalyst modifies the electric field generation and distribution and also the electron energy distribution resulting in more generation of reactive species; molecules, free radicals, excited species, atoms, ions and electrons. These species then react on the catalyst surface resulting in more conversion and selectivity. The presence of the catalyst in the discharge gap between the electrodes provides the surface for the development of the plasma and would be dependent on the dielectric properties of the catalyst packing material [58]. It has been suggested that, energy is concentrated in the gaps and pores of the catalyst resulting in more electron impact excitation, dissociation and ionization and also more collision of electrons and adsorbed species on the catalyst. The presence of the active Ni-metal of the catalyst enhances selective reforming and cracking reactions

The detailed gas composition in relation to catalysis alone, plasma alone, plasma-catalysis, plasma steam reforming and plasma catalytic steam reforming are shown in Figure 3. Figure 3(a) shows that the hydrogen gas yield obtained with catalyst alone was 0.19 mmol $g^{-1}_{plastic}$ with methane yield at 0.26 mmol $g^{-1}_{plastic}$. The use of plasma alone increased the yield of hydrogen to 1.10 mmol $g^{-1}_{plastic}$, while methane increased to 0.56 mmol $g^{-1}_{plastic}$. Figure 3(b) shows the analysis of the individual C_2 – C_4 hydrocarbons. Total C_2 – C_4 hydrocarbons were 1.66 mmol $g^{-1}_{plastic}$ for pyrolysis-catalysis and when the plasma alone was used, the total C_2 – C_4 hydrocarbons increased to 2.23 mmol $g^{-1}_{plastic.}$ The individual hydrocarbons (Figure 3(b) shows that the alkene gases all showed an increase when the plasma was used. The use of plasma has enhanced the production of the gases by cracking the fragments of the polyethylene polymer chain produced from pyrolysis, producing mainly ethene and also propene and butene. The increase in the yield of hydrogen gas (Figure 3(a) was more significant which suggests the plasma has cracked more of the C-H bonds. Nickel catalysts are known for their activity in cracking tars in pyrolysis-gasification reactions. Addition of the 10 wt.% Ni/Al_2O_3 catalyst to the plasma process (plasma-catalysis) showed an increase in the hydrogen yield to 1.50 mmol $g^{-1}_{plastic}$. When steam was used for plasma reforming without catalyst, a higher yield of hydrogen was obtained at 2.27 mmol $g^{-1}_{plastic}$ but no CO was detected. Plasma catalytic steam reforming generated hydrogen at 4.56 mmol $g^{-1}_{plastic}$ and CO at 0.50 mmol $g^{-1}_{plastic}$with a decrease in the methane yield. Figure 3(b) shows that the C_2 – C_4 hydrocarbons were decreased in concentration, particularly with the introduction of steam, resulting in steam reforming and catalytic steam reforming of the pyrolysis hydrocarbons, suggesting enhanced steam reforming of the methane and hydrocarbons in the presence of the Ni/Al_2O_3 catalyst (Eq. 4). The reaction also produced CO_2 at 0.5 mmol $g^{-1}_{plastic}$ (Figure 3(a)) suggesting that in addition to steam reforming, the catalyst also promoted water gas shift reaction (Eq. 5) to increase the hydrogen yield. It has been proposed that in the gas phase, the plasma causes the dissociation of the hydrocarbons into radicals (Eq. 6) [52] and the injected steam into H and OH radicals (Eq. 7) [48]. On the catalyst surface, the CH_x radicals generated in the plasma and adsorbed on the catalyst surface undergo further dissociation into adsorbed carbon and adsorbed hydrogen. On the other hand, adsorbed oxygen was formed from the oxygen species from the injected steam. The adsorbed carbon and adsorbed oxygen reacted on the catalyst surface forming adsorbed CO (Eq. 8) which is subsequently released as CO, while adsorbed hydrogen recombine with adsorbed hydrogen or CH_x radicals to produce hydrogen gas (Eq. 9).

$$C_nH_m + nH_2O \rightarrow (n + m/2)H_2 + nCO \quad (4)$$

$$CO + H_2O \rightarrow H_2 + CO_2 \quad (5)$$

$$C_nH_m \rightarrow CH_x + H \quad (6)$$

$$H_2O \rightarrow H + OH \quad (7)$$

$$C_{ads} + O_{ads} \rightarrow CO_{ads} \quad (8)$$

$$H_{ads} + H_{ads} \rightarrow H_{2ads} \quad (9)$$

Influence of plasma power input on the pyrolysis-plasma process. Table 2 shows the gas yield from the pyrolysis-plasma processing of waste polyethylene for a number of different process parameters. The influence of power input to the plasma on the pyrolysis-plasma process was investigated at input powers of 20 W, 40 W and 60 W and the results are shown in Table 2. The input power was adjusted by changing the applied voltage through a voltage regulator at constant applied frequency of 1500 Hz. The experiments were carried out by pyrolysis of the HDPE to a final pyrolysis temperature of 500 °C in the first stage and using plasma alone with different power inputs, without catalyst or steam, in the second stage. The results were compared with the result of the one-stage pyrolysis of the HDPE carried out at 500 °C without any accompanying second-stage. A total gas yield of 5.4 wt.% was obtained from the pyrolysis of HDPE at 500 °C with a liquid yield (mostly wax) of 87.0 wt.%. When a second stage plasma reactor was incorporated into the system and a plasma discharge generated at a power input of 20 W, the gas yield increased to 9.6 wt.%. This was due to the active species generated in the plasma that caused the cracking of the pyrolysis gases and higher molecular weight hydrocarbons. This was also confirmed by the reduction in the liquid yield from 87.0 wt % to 78.0 wt.%. When the input power was increased to 40 W, the gas yield increased to 10.3 wt.% and then to 10.9 wt.%. with a further increase in the input power to 60 W. This may be attributed to the enhanced electric field and higher electron density of the plasma discharge when the input power was increased, promoting more reaction species for cracking the hydrocarbons. More active species and radicals are generated at higher discharge power, creating a more reactive environment that enhances conversion rate of the gases [59]. Tu and Whitehead [28] investigated the effect of discharge power on the dry reforming of methane in a DBD reactor and observed that the conversion increased linearly with increasing discharge power. They also observed that at higher discharge power, more syngas was produced.

The gas composition obtained from the different plasma input power are shown in Figure 4. Compared to the one stage pyrolysis process, the introduction of the non-thermal plasma in the second stage significantly improved the hydrogen yield which increased further with an increase in the plasma input power (Figure 4(a). For example, 0.63 mmol $g^{-1}_{plastic}$ of hydrogen was produced at 20 W, 0.84 $g^{-1}_{plastic}$ produced at 40 W and 1.04 $g^{-1}_{plastic}$ was produced at 60 W. This is attributed to the enhanced electric field and electron density when the input power was increased. No carbon oxide was produced in this set of experiments because there was no oxygen source as only pure nitrogen was used in generating the plasma.

Figure 4(b) shows the yields of the individual C_2 — C_4 hydrocarbon gases. Increasing input power to the plasma showed an increase in hydrocarbon gases, suggesting enhanced cracking of the pyrolysis gases. At 60 W plasma power input, there was a slight decrease in the yields of the hydrocarbons which may be due to further cracking to produce more methane and hydrogen as reflected in Figure 4(a)

Influence of metal catalyst type on the pyrolysis-plasma process: The influence of different metal catalysts on the hydrogen production from the pyrolysis-plasma catalysis (no steam input) of HDPE was investigated. Four different transition metal catalysts were used, Ni/Al_2O_3, Fe/Al_2O_3, Cu/Al_2O_3 and Co/Al_2O_3 each with a 10 wt. % metal loading and prepared using a calcination temperature of 750 °C. The experiments were carried out with 1g of the catalyst placed in the centre of the discharge region which was sustained at an input power of 60 W. The results for the product gas yield over the different metal-alumina catalysts are shown in Table 2. The highest gas yield of 12.0 wt. % was produced with the Ni/Al_2O_3 catalyst. In terms of the total gas yield produced, the order of the catalysts used was $Ni/Al_2O_3 > Co/Al_2O_3 > Fe/Al_2O_3 > Cu/Al_2O_3$. Moreover, the liquid oil/wax yield produced from the pyrolysis of the polyethylene decreased with increasing gas yield. The gas composition from the different metal-alumina catalysts is shown in Figure 5. Figure 5(a) shows that the highest hydrogen gas yield of 1.5 mmol $g^{-1}_{plastic}$ was obtained with Ni/Al_2O_3 followed by Co/Al_2O_3 with 1.36 mmol $g^{-1}_{plastic}$. Figure 5(b) shows the yield of C_2 — C_4 hydrocarbons with the different catalysts and shows that they were very similar irrespective of what catalyst was used.

The results show that coupling the plasma with the different catalysts has enhanced the product yield because the catalysts influence the discharge properties which influence the reaction between the plasma excited species and the pyrolysis gases. The discharge mode changed from filamentary for plasma alone to a combination of filamentary and surface discharge in the plasma-catalytic process. It has been suggested that for the case of plasma-catalysis there is a possibility of direct Eley-Rideal reaction of the adsorbed species on the catalysts and the gas phase plasma-generated radicals thus producing additional reaction pathways with lower energy barriers and higher rates than conventional catalysis [29]. The activities of the different catalysts also depend on their chemical activities and dielectric properties.

To test the activity of the four catalysts for low temperature catalytic steam reforming in the presence of plasma, a steam input of 2 g h^{-1} $g^{-1}_{catalyst}$ into the second stage catalytic plasma process was used. The results of the gas yield and gas composition are shown in Table 2 and Figure 6, respectively. Table 2 shows that for each of the catalysts used an enhanced gas yield was obtained with the pyrolysis-catalytic steam reforming process indicating a contribution from the injected steam. For example, with the introduction of steam, gas yield increased from 12.0 wt.% to 17.8 wt.% using Ni/Al_2O_3, from 11.2 wt.% to 15.6 wt.% using Fe/Al_2O_3, 10.9 wt.% to 14.8 wt.% using Cu/Al_2O_3 and 11.4 wt.% to 16.6 wt.% using Co/Al_2O_3.

Figure 6(a) shows that compared to plasma-catalysis (Figure 5), the yield of hydrogen was significantly increased for all the catalysts for the pyrolysis-plasma catalytic steam reforming of polyethylene. This, in addition to the production of CO indicated that steam reforming reactions took place with all the catalysts according to Eq. 4. The hydrogen yield also followed the trend for total gas yield with Ni/Al_2O_3 producing the highest hydrogen yield at 3.52 mmol $g^{-1}_{plastic}$. Figure 6(b) shows that for the C_2 — C_4 hydrocarbons, the Ni/Al_2O_3 catalyst also gave the lowest yield of hydrocarbons suggesting they have been reformed using the steam to produce more syngas. This higher performance of the Ni/Al_2O_3 is attributed to its better activity in cracking both C – C and C – H bonds [60]. The CH_4 and C_2 — C_4 hydrocarbon yields for the Fe/Al_2O_3, Cu/Al_2O_3 and Co/Al_2O_3 catalysts were all very similar.

Influence of steam input on the pyrolysis-plasma process: The influence of different steam inputs on the plasma catalytic steam reforming process was investigated using different steam input rates (0, 2, and 6 g h^{-1} $g^{-1}_{catalyst}$) with a plasma input power of 60 W using the Ni/Al_2O_3 catalyst. Table 2 shows the gas yields obtained with the different steam input rates including zero steam injection. At 0 g h^{-1} $g^{-1}_{catalyst}$ (no steam), 12.0 wt.% of total gas was obtained, however, with the introduction of steam to the plasma-catalytic at 2 g h^{-1} $g^{-1}_{catalyst}$, a significant increase in the gas yield was observed at 17.8 wt.%. This shows that the introduction of steam into the system has promoted the conversion of pyrolysis volatiles to produce more gas. It has been reported that when steam is introduced in the discharge region, OH radicals are generated through electron-impact dissociation of water and collisions of the water with excited N_2 species [61]. These radicals leading to increased conversion of the pyrolysis volatiles. A further increase in the gas yield to 19.8 wt % was obtained at the higher steam input of 4 g h^{-1} $g^{-1}_{catalyst}$ indicating that more water has reacted with the pyrolysis gases to generate more gas. However, at 6 g h^{-1} $g^{-1}_{catalyst}$ steam input, the gas yield decreased to 14.2 wt.%.

The gas yield for the product gases is shown in Figure 7 and shows that introducing steam resulted in a marked increase in hydrogen yield (Figure 7(a). The hydrogen yield increased from 1.5 mmol $g^{-1}_{plastic}$ in the absence of steam to 3.52 mmol $g^{-1}_{plastic}$ when steam was introduced at 2 g h^{-1} $g^{-1}_{catalyst}$. Increasing the steam input to 4 g h^{-1} $g^{-1}_{catalyst}$ resulted in further increase in the hydrogen yield to 4.56 mmol $g^{-1}_{plastic}$ but at higher steam input of 6 g h^{-1} $g^{-1}_{catalyst}$, the hydrogen yield decreased to 3.24 mmol $g^{-1}_{plastic}$. It is also noteworthy that no CO was detected in the absence of steam but when steam was added CO was obtained. The initial increase of the steam input from 2 g h^{-1} $g^{-1}_{catalyst}$ to 4 g h^{-1} $g^{-1}_{catalyst}$ promoted the steam reforming of the pyrolysis hydrocarbons resulting in enhanced hydrogen and CO yields while at higher steam flow rate the yields decreased suggesting there is an optimum steam:carbon ratio for maximum hydrogen yield. Liu et al. [62] studied the effect of steam:carbon ratio on the steam reforming of toluene in a gliding arc discharge and reported the best performance of the reactor at a steam:carbon ratio of between 2 - 3. When steam was added, high activity radicals such as OH are generated in the discharge zone which provide a route for the hydrocarbons conversion. When the steam input was increased, the concentration of the OH radicals increased and a corresponding increase in the yield of H_2 and CO was observed. At 4 g h^{-1} $g^{-1}_{catalyst}$, the extra steam was also able to promote the water gas shift reaction (Eq. 5) resulting in the production of CO_2 and increased yield of hydrogen gas. Sugasawa et. al. [63], noted that increased water content increased the oxidative capacity of water to promote CO_x production. However, beyond the optimum steam:carbon ratio, there is an excess of steam which could be adsorbed on the surface of the catalyst, thereby reducing the contact of the hydrocarbons with the catalyst [64]. Excess water in the plasma can also result in a reduced density of energetic electrons as a result of electron attachment to water molecules [65]. A number of studies have reported quenching of the reactive chemical species when the amount of water in the plasma is in excess [66-68].

The maximum hydrogen yield obtained from the pyrolysis-plasma catalytic steam reforming of waste high density polyethylene was only 4.56 mm g^{-1}. Conventional pyrolysis-catalytic steam reforming has shown much higher yields of hydrogen from waste plastics. For example, Yao et al [69] reported a hydrogen yield produced from the two-stage fixed bed pyrolysis-catalytic steam reforming of polyethylene of 66 mmol $g^{-1}_{plastic}$. A hydrogen yield of 88 mmol $g^{-1}_{plastic}$was reported for polypropylene using a two-stage screw kiln reactor followed by a fixed bed catalytic steam reforming reactor [70]. Czernik and French [13] used a continuous two-stage fluidised bed pyrolysis reactor with a fluidised bed catalytic steam reforming reactor for the processing of polypropylene and reported a hydrogen yield of 168mmol $g^{-1}_{plastic}$. Barbarias et al [17] produced even higher yields of hydrogen using a continuous fluidised spouted bed reactor with a coupled fluidised bed catalytic steam reforming reactor. They reported a hydrogen yield from the pyrolysis-catalytic steam reforming of polyethylene of 185 mmol $g^{-1}_{plastic}$. The yield of hydrogen will be influenced by the reactor design, for example a fluidised bed will provide enhanced heat and mass transfer of reactants compared to a fixed bed reactor, the catalytic steam reforming temperature, the type of catalyst used, steam input, catalyst:plastic ratio etc. [71]. However, the comparative low yield from the pyrolysis-plasma catalytic process in the work reported here is produced at significantly lower catalyst temperature of 250 °C compared to typical thermal reforming catalyst temperatures of ~800 °C. Comparison of the energy balance of the two processes for the production of hydrogen from plastics would enable a definitive assessment of the advantages of low-temperature plasma-catalytic steam reforming. In addition, the Ni/Al_2O_3 catalysts used in this work that produced the highest hydrogen yield is designed for thermal catalytic steam reforming at high temperature and would be significantly less efficient at the operational temperature of the plasma reactor (250 °C). Therefore, catalysts should be designed for the unique plasma-catalytic environment, for example support materials with enhanced dielectric properties which promote plasma formation and active metal species that promote reforming catalytic activity and selectivity for hydrogen production in the plasma environment.

CONCLUSIONS

The use of a novel two stage pyrolysis-non thermal dielectric barrier discharge (DBD) plasma reactor has been studied for hydrogen production from waste high density polyethylene. The results showed that using a DBD plasma enhanced the total gas and hydrogen yield compared to catalysis alone. When a Ni/Al_2O_3 catalyst was incorporated in the discharge region, the yields of all the product gases increased due to the synergistic effect of plasma and catalyst. Introducing steam into the plasma promoted steam reforming reactions due to the formation of OH radicals that open a new reaction route resulting in increased production of hydrogen and carbon monoxide.

Increasing the plasma power input from 20 W to 60 W increased the electric field and electron density resulting in increased hydrogen yield from 0.63 mmol $g^{-1}_{plastic}$ to 1.10 mmol $g^{-1}_{plastic}$. In addition, the total gas yield also increased. Four different transition metal catalysts (Ni/Al_2O_3, Co/Al_2O_3, Fe/Al_2O_3 and Cu/Al_2O_3) were investigated for the plasma catalysis and plasma catalytic steam reforming process and Ni/Al_2O_3 gave the highest yield of total gas and hydrogen gas. The effect of steam input rate was further studied using the Ni/Al_2O_3 catalyst. When steam was injected, OH radicals were produced and their concentration increased with increased steam input rate up to an optimum steam:carbon ratio. At the optimum steam input rate of 4 g h^{-1} $g^{-1}_{catalyst}$, the highest hydrogen gas yield was obtained as 4.56 mmol $g^{-1}_{plastic}$. When the steam input was increased to 6 g h^{-1} $g^{-1}_{catalyst}$, the hydrogen yield was reduced due to saturation of the catalyst and quenching of plasma species.

This study shows that the two-stage pyrolysis-non-thermal plasma reactor can be used for the conversion of waste HDPE to produce hydrogen gas at low temperature and atmospheric pressure. Although the hydrogen yield is low compared to thermal catalytic processes, the low temperature used in this system can be seen as an alternative route for hydrogen production from the waste HDPE. A techno-economic assessment of the pyrolysis-non-thermal plasma catalysis process should be compared with that of conventional thermal catalytic processes to ascertain the potential of the process, in terms of mass and energy balance, and cost.

REFERENCES

[1] Williams, P.T., Waste Treatment and Disposal. 2005, Chichester: John Wiley & Sons, Ltd.

[2] Agency, E.E., Preventing plastic waste in Europe, in EEA Report 2019. 2019.

[3] Geyer, R., Jambeck J., Law K., Production, use, and fate of all plastics ever made. *Sci. Adv.,* **2017,** 3(7), e1700782.

[4] Hahladakis, J., Velis C.A., Weber R., Ilacovidou E., Purnell P., An overview of chemical additives present in plastics: Migration, release, fate and environmental impact during their use, disposal and recycling. *J. Hazard. Mat.,* **2018**, 344, 179-199.

[5] Jambeck, J.R., Geyer R., Wilcox C., Siegler T.R., Perryman M., Andrady A., Narayan R., Law K.L., Plastic waste inputs from land into the ocean. *Science*, **2015**. 347(6223), 768-771.

[6] PlasticsEurope, Plastics-the Facts 2019. Plastics Europe, 2019.

[7] Demirbaş, A., Pyrolysis of municipal plastic wastes for recovery of gasoline-range hydrocarbons. *J. Anal. Appl. Pyrolysis*, **2004**, 72(1), 97-102.

[8] Urionabarrenechea A.L., Marco I., Caballero B.M., Laresgoiti M.F.,., Pyrolysis of municipal plastic wastes: Influence of raw material composition. *Waste Manag.,* **2010**, 30(4), 620-627.

[9] Cho M.H., Mun T.Y., Kim J.S., Production of low-tar producer gas from air gasification of mixed plastic waste in a two-stage gasifier using olivine combined with activated carbon. *Energy*, **2013.** 58, 688-694.

[10] Wilk, V., Hofbauer H., Conversion of mixed plastic wastes in a dual fluidized bed steam gasifier. *Fuel*, **2013**, 107, 787-799.

[11] Barbarias I., Lopez G., Alvaerz J., Artetxe M., Arregi A., Bilbao J., Olazar M. A sequential process for hydrogen production based on continuous HDPE fast pyrolysis and in-line steam reforming. *Chem. Eng. J.,* **2016**, 296, 191-198.

[12] Arregi A., Lopez G., Amutio M., Artetxe M., Barbarias I., Bilbao J., Olazar M., Role of operating conditions in the catalyst deactivation in the in-line steam reforming of volatiles from biomass fast pyrolysis. *Fuel*, **2018**, 216, 233-244.

[13] Czernik, S., French R., Production of hydrogen from plastics by pyrolysis and catalytic steam reform. *Energ. Fuels*, **2006,** 20, 754-758.

[14] Namioka, T., Saito A., Inoue H. Park Y., Min T. Roh S. Yoshikawa K., Hydrogen-rich gas production from waste plastics by pyrolysis and low-temperature steam reforming over a ruthenium catalyst. *Appl. Energ.* **2011**, 88(6), 2019-2026.

[15] Acomb, J.C., Wu C., Williams P.T., The use of different metal catalysts for the simultaneous production of carbon nanotubes and hydrogen from pyrolysis of plastic feedstocks. *Appl. Cat. B-Environ.,* **2016**, 180, 497-510.

[16] Barbarias, I., Lopez G., Artetxe M., Arregi A., Santamaria L., Bilbao J., Olazar M., Pyrolysis and in-line catalytic steam reforming of polystyrene through a two-step reaction system. *J. Anal. Appl. Pyrolysis*, **2016,** 122, 502-510.

[17] Barbarias, I., Lopez G., Artetxe M., Arregi A., Santamaria L., Bilbao J., Olazar M, Valorisation of different waste plastics by pyrolysis and in-line catalytic steam reforming for hydrogen production. *Energ. Conv. Manag*. **2018**, 156, 575-584.

[18] Arregi, A., Amutio M., Lopez G., Artetxe M., Alvaerz J., Barbarias I., Bilbao J., Olazar M., Hydrogen-rich gas production by continuous pyrolysis and in-line catalytic reforming of pine wood waste and HDPE mixtures. *Energ. Conv. Manag.* **2017**, 136, 192-201.

[19] Morozov, A.I., Introduction to Plasma Dynamics. 2012, Boca Raton, FL: C.R.C. Press.

[20] Gallagher, M.J., Fridman A., Plasma reforming for H_2-rich synthesis gas, in Fuel Cells: Technologies for Fuel Processing, D. Shekhawat, J.J. Spivey, and D.A. Berry, Editors. 2011, Elsevier: Amsterdam. p. 223-259.

[21] Fridman, A., Plasma Chemistry. 2008, New York: Cambridge University Press.

[22] Fridman, A., Nester S., Kennedy L.A., Saveliey S., Yardimici O.M., Gliding arc gas discharge. *Prog. Energ. Combust. Sci.* **1999**, **25**, 211-231.

[23] Mei, D. , Tu X., Conversion of CO_2 in a cylindrical dielectric barrier discharge reactor: Effects of plasma processing parameters and reactor design. *J. CO2 Utiliz*., **2017,** 19, 68-78.

[24] Diaz, L., Zhang K., Phan A., Monomer recovery through advanced pyrolysis of waste high density polyethylene (HDPE). *RSC Green Chem.,* **2018**, 20, 1813-1823.

[25] Kalra, C.S., Gutsol A.F., Fridman A., Gliding arc discharges as a source of intermediate plasma for methane partial oxidation. *IEEE Trans. Plasma Sci.,* **2005**, 33(1), 32-41.

[26] Paulussen, S., Verheyde B. Tu X. De Bie C. Martens T., Petrovic D., Bogaerts A. Sels B. Conversion of carbon dioxide to value-added chemicals in atmospheric pressure dielectric barrier discharges. *Plasma Sourc. Sci. Technol*., **2010.** 19(3).

[27] Xu, S., Khalaf P.I., Martin P.A., Whitehead C.J., CO_2 dissociation in a packed-bed plasma reactor: effects of operating conditions. *Plasma Sourc. Sci. and Technol.* **2018**, 27(7).

[28] Tu, X., Whitehead J., Plasma-catalytic dry reforming of methane in an atmospheric dielectric barrier discharge: Understanding the synergistic effect at low temperature. *Appl. Cat. B-Environ*., **2012**, 125, 439-448.

[29] Whitehead, J., Plasma-catalysis: The known knowns, the known unknowns and the unknown unknowns. *J. Phys. D-Appl. Phys.,* **2016,** 49(24), 1-24.

[30] Wang, L., Yi Y., Wu C., Guo H., Tu X., One-step reforming of CO_2 and CH_4 to high-value liquid chemicals and fuels at room temperature by plasma-driven catalysis. *Angew. Chem. Intl. Ed.,* **2017**, 56, 13679-13683.

[31] Chen, H.-L., Lee H.M., Chen S.H., Chao Y., Chang M.B., Review of plasma catalysis on hydrocarbon reforming for hydrogen production—Interaction, integration, and prospects. *Appl. Cat. B-Environ.*, **2008,** 85(1-2), 1-9.

[32] Whitehead, J., Plasma catalysis: A solution for environmental problems. *Pure Appl. Chem*, 2010. **82**(6): p. 1329-1336.

[33] Zeng, Y., Mei D., Tu X., Plasma-catalytic dry reforming of CH4 and CO2: effect of bimetallic catalysts, in *22nd International Symposium on Plasma Chemistry.* **2015:** Antwerp, Belgium.

[34] Tao, K., Ohta N., Liu G., Yoneyama Y., Wang T., Tsubali N., Plasma enhanced catalytic reforming of biomass tar model compound to syngas. *Fuel,* **2010,** 104, 53-57.

[35] Tu, X., Gallon H.J., Twigg M.V., Gorry P.A., Dry reforming of methane over a Ni/Al_2O_3 catalyst in a coaxial dielectric barrier discharge reactor. *J. Phys. D-Appl. Phys.,* **2011,** 44, 274007.

[36] Sentek, J., Krawczyl K., Miotek M., Kalczewska M., Krokei T., Koi T., Schenk A., Gericke K.H., Szalowski K.S., Plasma-catalytic methane conversion with carbon dioxide in dielectric barrier discharges. *Appl. Cat. B-Environ.,* **2010,** 94(1-2), 19-26.

[37] Lu, N., Zhang C., Shang K., Jiang N., DBD plasma assisted CO_2 conversion: understanding the effects of reactor design and operating parameters. J *J. Phys. D-Appl. Phys.,* **2019**, 52.

[38] Khoja, A., Tahli M, Aishah N., Amin S., Javed A., Mehran M.T, Kinetic study of dry reforming of methane using hybrid DBD plasma reactor over La2O3 co-supported Ni/MgAl2O4 catalyst. *Int. J. Hydrogen Energ.,* **2020**, **45**, 12256-12271.

[39] Li, M.W., Xu G.H., Chen L., Fu H.F., Carbon dioxide reforming of methane using DC corona discharge plasma reaction. *J. Phys. Chem.* A, **2004,** 108(10), 1687-1693.

[40] Aziznia, A., Bozorgzadeh H.R., Matin N.S., Baghalha M., Mohamadlizadeh A., Comparison of dry reforming of methane in low temperature hybrid plasma-catalytic corona with thermal catalytic reactor over Ni/γ-Al2O3. *J. Natural Gas Chem.,* **2012**, 21(4), 466–475.

[41] Wang, W., Mei D., Tu X., Bogaerts A., Gliding arc plasma for CO2 conversion: Better insights by a combined experimental and modelling approach. *Chem. Eng. J.*, **2017**, 330, 11-25.

[42] Wu, A., Yan J., Zhang H., Zhang M., Du C., Li X., Study of the dry methane reforming process using a rotating gliding arc reactor. *Int. J. Hydrogen Energ*. **2014**, 39(31), 17656–17670.

[43] Li, D., Li X., Bai. M., Tao X., Shang S., Dai X., Yin Y., CO_2 reforming of CH4 by atmospheric pressure glow discharge plasma: A high conversion ability. *Int. J. Hydrogen Energ*., **2009,** 34(1), 308-313.

[44] Cheng, D.G. Zhu X., Ben Y., He F., Cui L., Liu C.J. Carbon dioxide reforming of methane over Ni/Al2O3 treated with glow discharge plasma. *Catal. Today*, **2006**, **115**(1), 205-210.

[45] Khoja, A., Tahir M., Amin N.A.S., Dry reforming of methane using different dielectric materials and DBD plasma reactor configurations. *Energ. Conv. Manag.,* **2017**, 144, 262-274.

[46] Zhang, K., Mukhirza T., Liu X., Greco P.P., Chiremba E., A study on CO2 and CH4 conversion to synthesis gas and higher hydrocarbons by the combination of catalysts and Dielectric-Barrier Discharges. *Appl. Cat. A-Gen.*, **2015**, 502, 138-149.

[47] Liu, S., Mei D.H., Nahil M.A., Gu S., Williams P.T., Tu X, Hybrid plasma-catalytic steam reforming of toluene as biomass tar model compound over Ni/Al2O3 catalysts. *Fuel Proc. Technol.,* **2017,** 166, 269-275.

[48] Liu, L., Wang Q., Song J., Ahmad S., Yang X., Sun Y., Plasma-assisted catalytic reforming of toluene to hydrogen rich syngas. *Catal. Sci. Technol.,* **2017**, **7**(18).

[49] Blanquet E., Nahil M.A., Williams P.T., Enhanced hydrogen-rich gas production from waste biomass using pyrolysis with non-thermal plasma-catalysis. *Catal. Today*, **2019**, 337, 216-224.

[50] Chung, W.C., Chang M., Review of catalysis and plasma performance on dry reforming of CH4 and possible synergistic effects. *Renew. Sus. Energ. Rev.,* **2016**, 62, 13-31.

[51] Neyts, E.C., Ostrikov K., Sunkara M.K., Bogaerts A., Plasma catalysis: Synergistic effects at the nanoscale. *Chem. Rev.,* **2015,** 115, 13408-13446.

[52] Mehta, P., Barboun P., Go D.B., Hicks J.C., Schneider W.F., Catalysis enabled by plasma activation of strong chemical bonds: A review. *ACS Energ. Lett.* **2019,** 4, 1115−1133

[53] Zhang, X., Cha M.S., Electron-induced dry reforming of methane in a temperature-controlled dielectric barrier discharge reactor. *J. Phys. D-Appl. Phys.,* **2013**, 46(41), 415205.

[54] Czernik, S., French R., Feik C., Chornet E., Hydrogen by catalytic steam reforming of liquid byproducts from biomass thermoconversion processes. *Ind. Eng. Chem. Res.,* **2002,** 41(17), 4209-4215.

[55] Nozaki, O. Muto M., Kadio S., Okazaki K., Dissociation of vibrationally excited methane on Ni catalyst: Part 2, Process diagnostics by emission spectroscopy. *Catal. Today,* **2004,** 89(1-2), 67-74.

[56] Fridman, A., Kennedy L.A., Plasma Physics and Engineering, 2nd edition. CRC Press. 2011. 324-325.

[57] Zeng, Y.X., Wang L., Wu F., Wang J.Q., Shen X., Tu X., Low temperature reforming of biogas over K-, Mg- and Ce-promoted Ni/Al_2O_3 catalysts for the production of hydrogen rich syngas: Understanding plasma-catalytic synergy. *Appl. Cat. B-Environ.,* **2018,** 224, 469-478.

[58] Neyts E.C., Bogaerts A., Understanding plasma catalysis through modelling and simulation-A review. *J. Phys. D: Appl. Phys.* **2014**, 47, 224010.

[59] JGallon J., Tu X., Whitehead J., Effects of reactor packing materials on H2 production by CO2 reforming of CH4 in a Dielectric Barrier Discharge. *Plasma Proc. Polym.,* **2012**, 9(1), 90-97.

[60] Hu, X., Lu G., Comparative study of alumina-supported transition metal catalysts for hydrogen generation by steam reforming of acetic acid. *Appl. Cat. B-Environ*., **2010**, 99(1-2), 289-297.

[61] Lim, M., Chun Y., Light tar decomposition of product pyrolysis gas from sewage sludge in a gliding arc plasma reformer. *Environ. Eng. Res.,* **2012**, 17(2), 89-94.

[62] Liu, S., Mei D., Wang L., Tu X., Steam reforming of toluene as biomass tar model compound in a gliding arc discharge reactor. *Chem. Eng. J.,* 2017, **307**, 793-802.

[63] Sugasawa, M., Terasawa T., Futamura S., Effects of initial water content on steam reforming of aliphatic hydrocarbons with nonthermal plasma. *J. Electrostatics,* **2010**. 68, 212–217.

[64] Liu, Y., Song J., Diao X., Liu L., Sun Y., Removal of tar derived from biomass gasification via synergy of non-thermal plasma and catalysis. *Sci. Total Environ* 2020, 137671.

[65] Yang, Y.C., Chun Y.N., Naphthalene destruction performance from tar model compound using a gliding arc plasma reformer. *Korean J. Chem. Eng.* **2011**, 28(2), 539-543.

[66] Zhang, H., Zhu F., Li X., Cen K., Du C. Tu X. , Rotating gliding arc assisted water splitting in atmospheric nitrogen. *Plasma Chem. Plasma Proc.,* 2016, 36(3).

[67] Bruggeman, P., Iza F., Guns P., Lauwers D., Kong M.G., Gonzalvo Y.A., Leys C., Schram D.C., Electronic quenching of OH(A) by water in atmospheric pressure plasmas and its influence on the gas temperature determination by OH(A–X) emission. *Plasma Sourc. Sci. Technol.,* **2009**, 19(1), 015016.

[68] Bruggeman, P., Schram D.C. Gonzalvo Y.A., Rego R., Kong M.G., Leys C., Characterization of a direct dc-excited discharge in water by optical emission spectroscopy. *Plasma Sourc. Sci. Technol.,* **2009**, 18(2), 025017.

[69] Yao D., Yang H., Chen H. Williams P.T., Investigation of nickel-impregnated zeolite catalysts for hydrogen/syngasproduction from the catalytic reforming of waste polyethylene. *Appl. Cat. B-Environ.,* **2018**, 227, 477-487.

[70] Wu C., Williams, P.T., Hydrogen from waste plastics by way of pyrolysis-gasification. *Waste Resour. Manag*., **2014**, 167, 35-46.

[71] Williams P.T., Hydrogen and carbon nanotubes from pyrolysis-catalysis of waste plastics: A review. *Waste Biomass Valor*., **2020**. https://doi.org/10.1007/s12649-020-01054-w.

FIGURE CAPTIONS

Figure 1. A schematic diagram of the two-stage pyrolysis-plasma reactor

Figure 2. Schematic diagram of the reactors

Figure 3. Comparison of gas composition from catalysis, plasma alone, plasma-catalysis, plasma steam reforming and plasma catalytic steam reforming processes. **3(a)** Main gas components, **3(b)** C_2 — C_4 hydrocarbons.

Figure 4. Influence of different plasma power input on the gas composition from pyrolysis-non-thermal plasma cracking of waste polyethylene (pyrolysis temperature 500°C, no steam, no catalyst). **4(a)** Main gas components, **4(b)** C_2 — C_4 hydrocarbons.

Figure 5. Influence of different metal catalysts on the gas composition from pyrolysis-plasma-catalysis of waste polyethylene (pyrolysis temperature 500°C, power 60 W, no steam). **5(a)** Main gas components, **5(b)** C_2 — C_4 hydrocarbons.

Figure 6. Influence of different metal catalysts on the gas composition from pyrolysis-plasma-catalytic steam reforming of waste polyethylene (pyrolysis temperature 500°C, power 60 W, steam WHSV 2 g h^{-1} $g^{-1}_{catalyst}$). **6(a)** Main gas components, **6(b)** C_2 — C_4 hydrocarbons.

Figure 7. Influence of different steam weight hourly space velocity on the total gas yield from pyrolysis-plasma-catalytic steam reforming of waste polyethylene (pyrolysis temperature 500°C, power 60 W, 10 wt. % Ni/Al_2O_3 catalyst). **7(a)** Main gas components, **7(b)** C_2 — C_4 hydrocarbons.

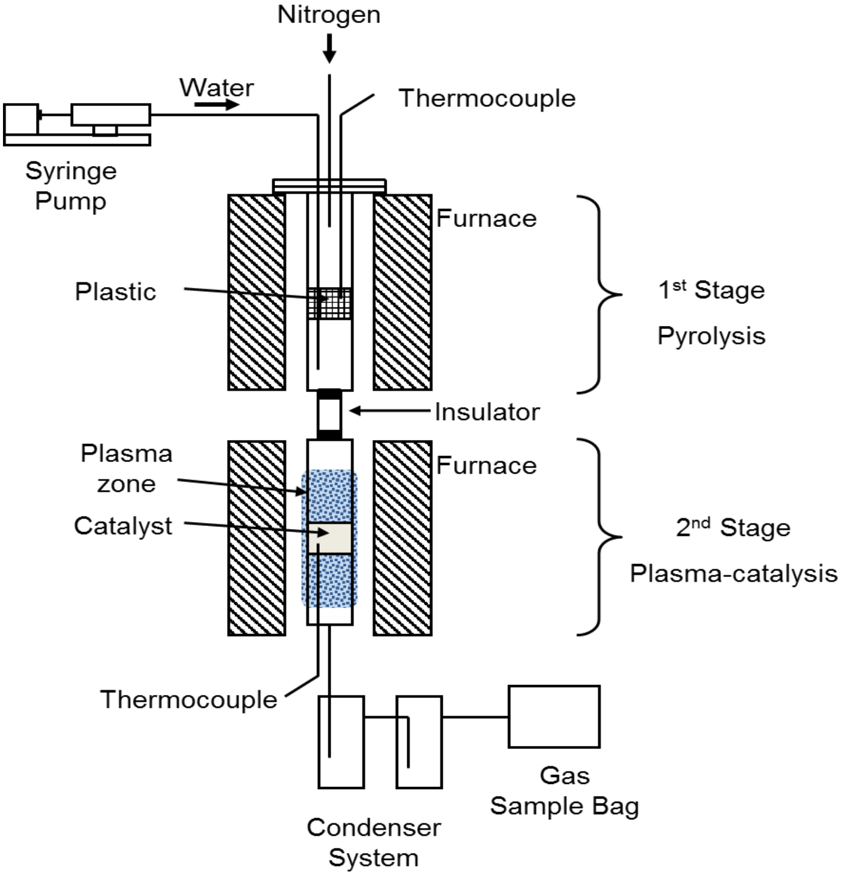

Figure 1. A schematic diagram of the two-stage pyrolysis-plasma reactor system

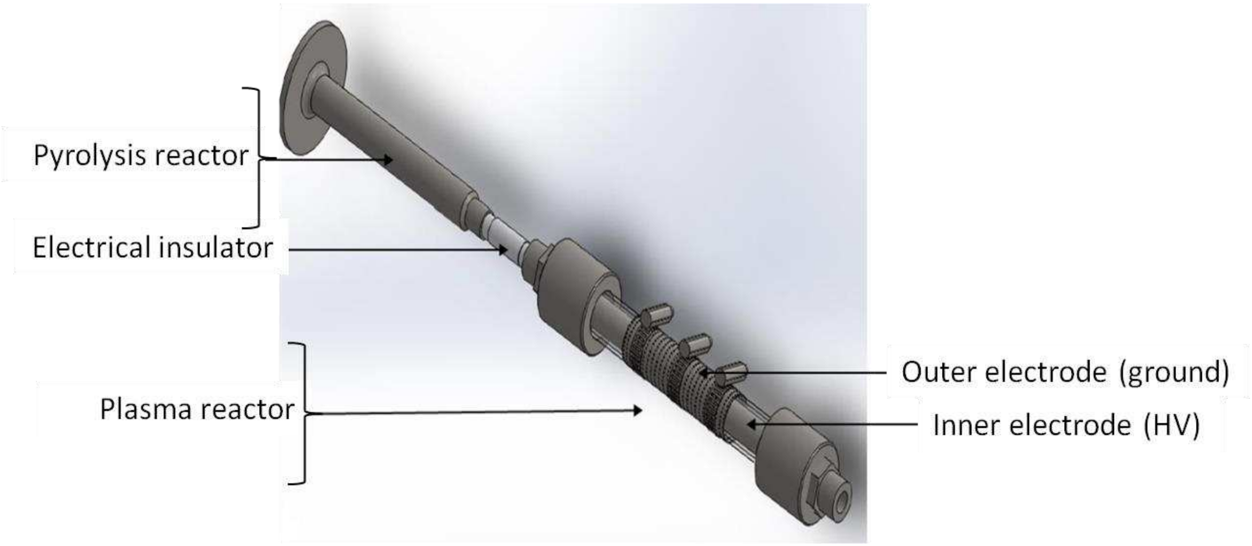

Figure 2. Schematic diagram of the reactors

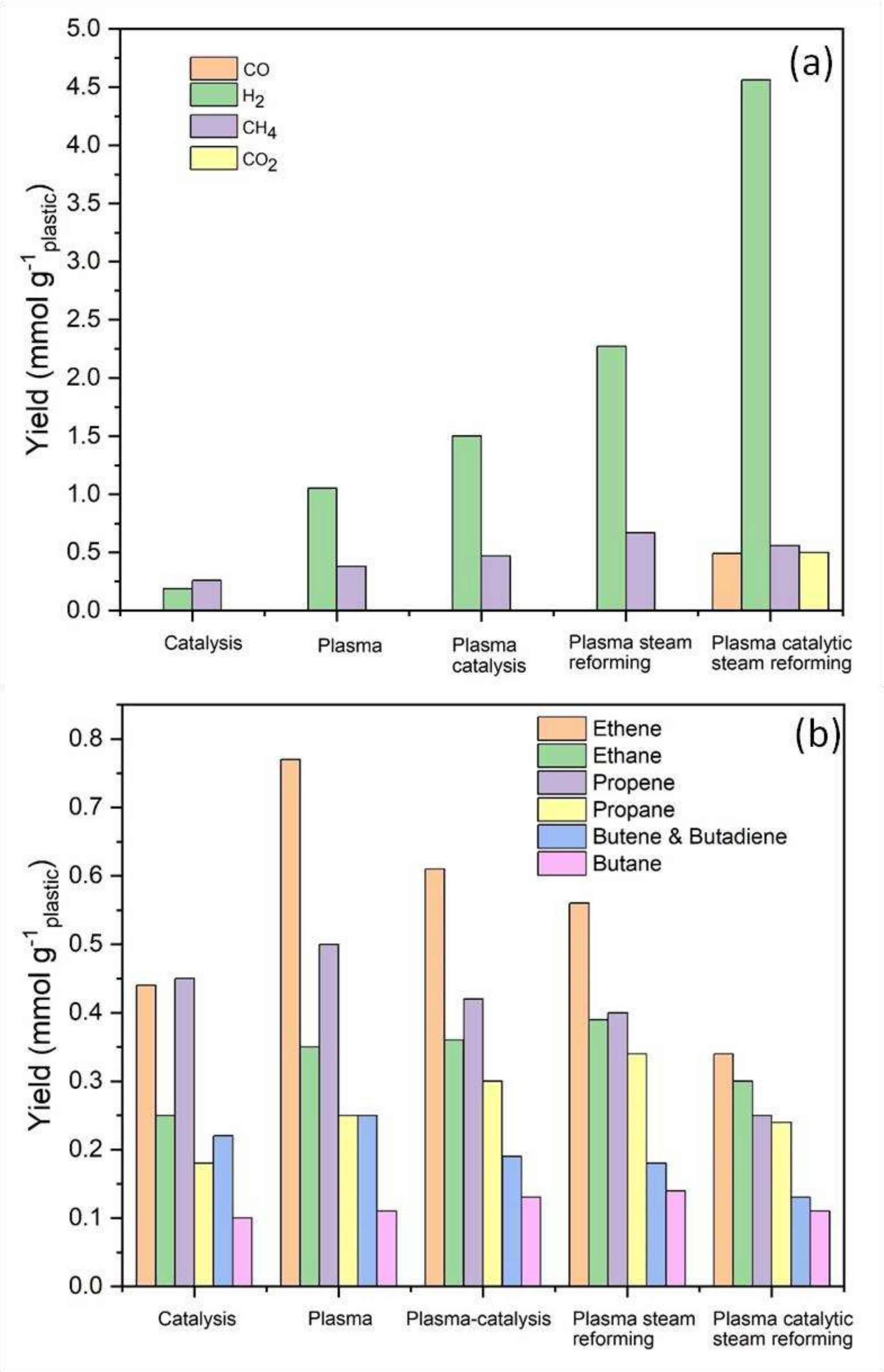

Figure 3. Comparison of the composition of lighter hydrocarbons from catalysis, plasma alone, plasma-catalysis, plasma steam reforming and plasma catalytic steam reforming processes. **3(a)** Main gas components, **3(b)** C_2 — C_4 hydrocarbons.

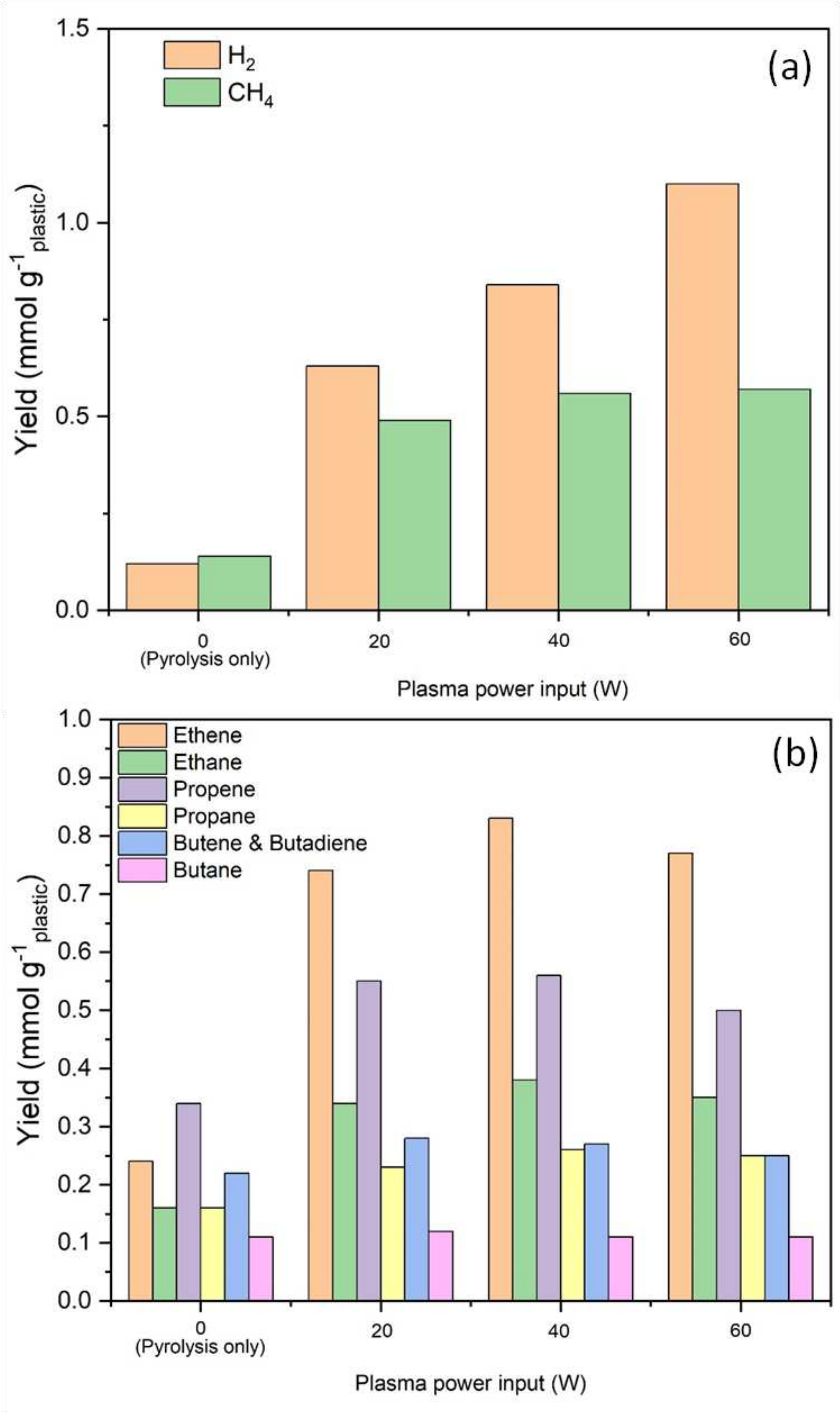

Figure 4. Influence of different plasma power input on the gas composition from pyrolysis-non-thermal plasma cracking of waste polyethylene (pyrolysis temperature 500°C, no steam, no catalyst). **4(a)** Main gas components, **4(b)** C_2 — C_4 hydrocarbons.

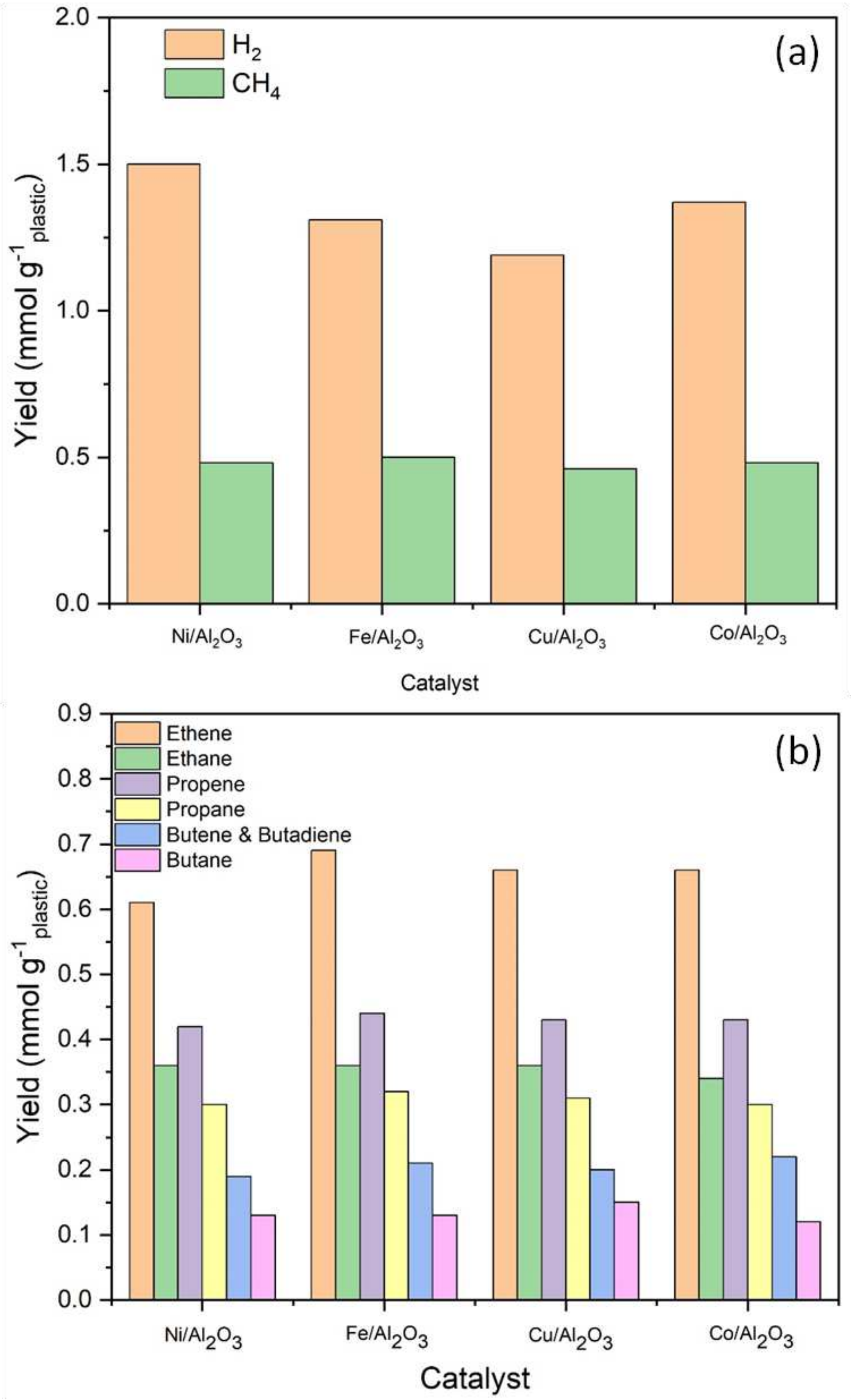

Figure 5. Influence of different metal catalysts on the gas composition from pyrolysis-plasma-catalysis of waste polyethylene (pyrolysis temperature 500°C, power 60 W, no steam). **5(a)** Main gas components, **5(b)** C_2 — C_4 hydrocarbons.

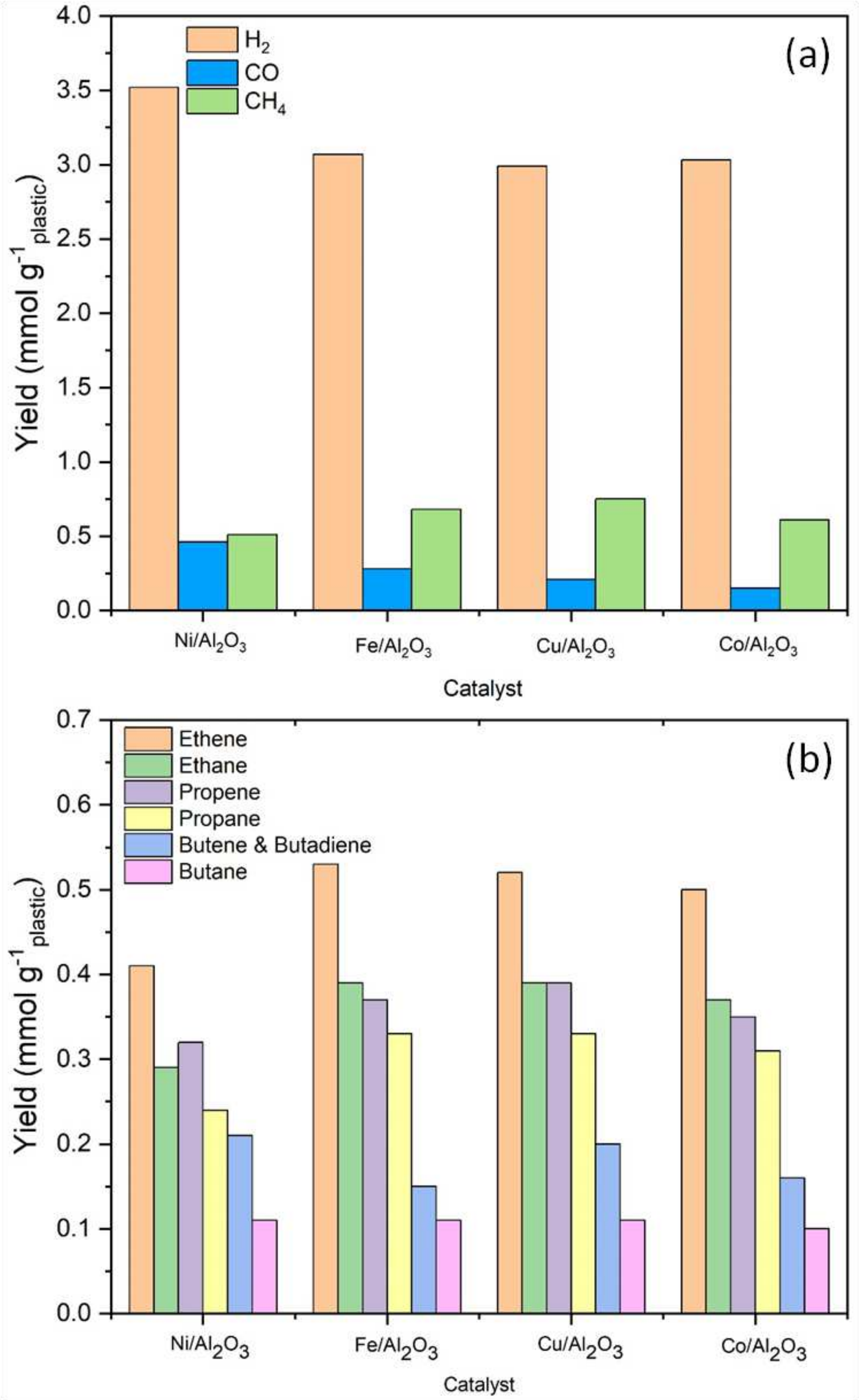

Figure 6. Influence of different metal catalysts on the gas composition from pyrolysis-plasma-catalytic steam reforming of waste polyethylene (pyrolysis temperature 500°C, power 60 W, steam WHSV 2 g h^{-1} $g^{-1}{}_{catalyst}$). **6(a)** Main gas components, **6(b)** C_2 — C_4 hydrocarbons.

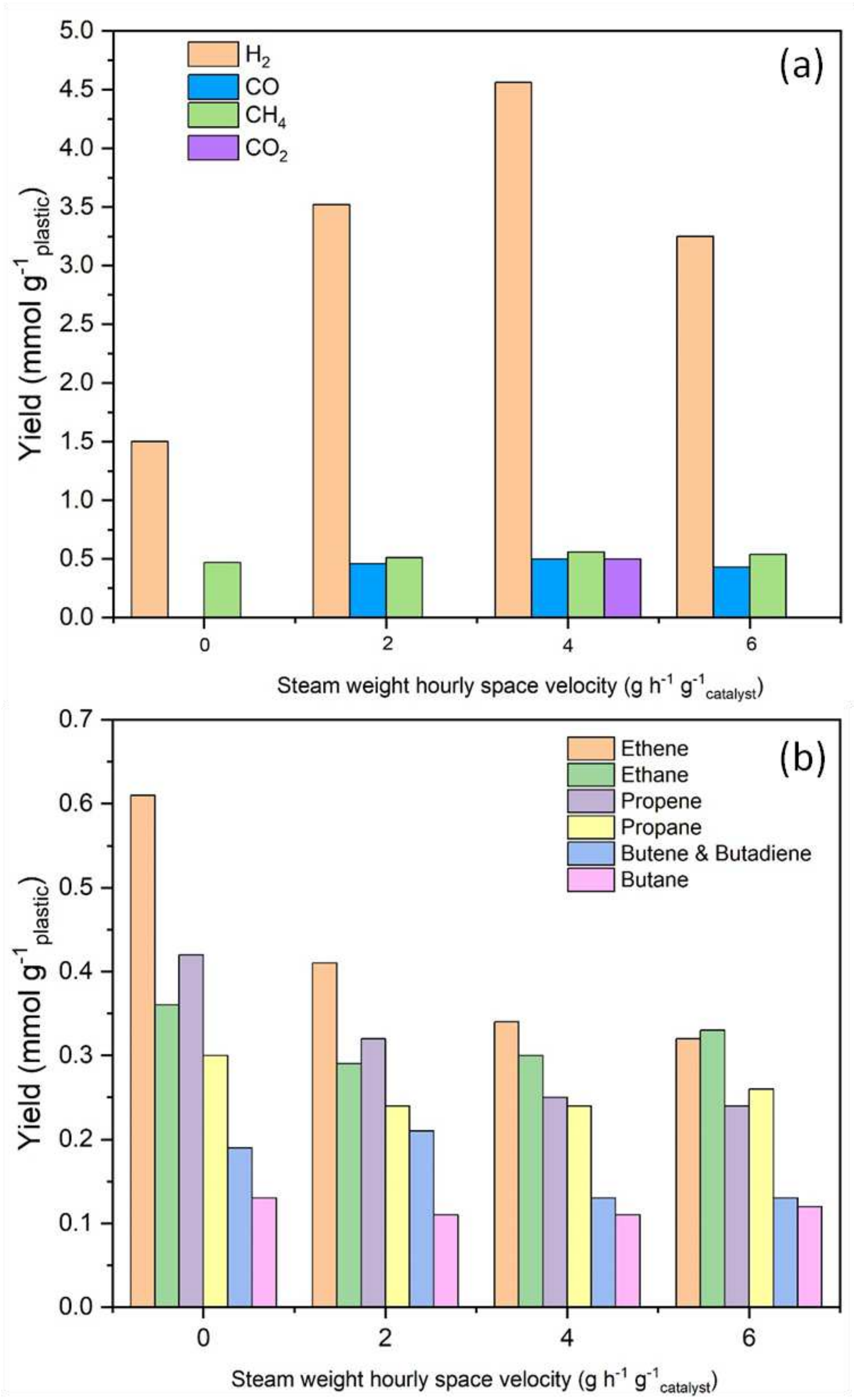

Figure 7a. Influence of different steam weight hourly space velocity on the gas composition from pyrolysis-plasma-catalytic steam reforming of waste polyethylene (pyrolysis temperature 500°C, power 60 W, 10 wt. % Ni/Al_2O_3 catalyst). **7(a)** Main gas components, **7(b)** C_2 — C_4 hydrocarbons.

Table 1. Comparison of total gas yield (in relation to the mass of plastic) from catalysis, plasma alone, plasma-catalysis, plasma steam reforming and plasma catalytic steam reforming processes.

	Catalysis	**Plasma alone**	**Plasma-catalysis**	**Plasma Steam reforming**	**Plasma catalytic steam reforming**
Gas yield (wt. %)	7.0	10.9	12.0	17.0	19.8

Table 2. Influence of various process parameters on the total gas yield from pyrolysis-non-thermal plasma processing of waste HDPE.

	Plasma input power (No catalyst)			
	0 W	20 W	40 W	60 W
Gas yield (wt.%)	5.4	9.6	10.3	10.9
	Catalyst type			
	Ni/Al_2O_3	Fe/Al_2O_3	Cu/Al_2O_3	Co/Al_2O_3
Gas yield (wt. %)	12.0	11.2	10.9	11.4
	Catalyst type with Steam input			
	Ni/Al_2O_3	Fe/Al_2O_3	Cu/Al_2O_3	Co/Al_2O_3
Gas yield (wt. %)	17.8	15.6	14.8	16.6
	Steam weight hourly space velocity (Ni/Al_2O_3) ($g\ h^{-1}\ g^{-1}_{catalyst}$)			
	0	2	4	6
Gas yield (wt. %)	12.0	17.8	19.8	14.2